Metals **2015**, *5*, 1315-1327; doi:10.3390/met5031315

OPEN ACCESS

metals

ISSN 2075-4701

www.mdpi.com/journal/metals/

Article

High Temperature Flow Response Modeling of Ultra-Fine Grained Titanium

Seyed Vahid Sajadifar and Guney Guven Yapici *

Mechanical Engineering Department, Ozyegin University, Istanbul 34794, Turkey;
E-Mail: seyedvahid.sajjadifar@ozu.edu.tr

* Author to whom correspondence should be addressed; E-Mail: guven.yapici@ozyegin.edu.tr;
Tel.: +90-216-564-9115; Fax: +90-216-564-9057.

Academic Editor: Heinz Werner Höppel

Received: 14 May 2015 / Accepted: 14 July 2015 / Published: 22 July 2015

Abstract: This work presents the mechanical behavior modeling of commercial purity titanium subjected to severe plastic deformation (SPD) during post-SPD compression, at temperatures of 600-900 °C and at strain rates of 0.001-0.1 s^{-1}. The flow response of the ultra-fine grained microstructure is modeled using the modified Johnson-Cook model as a predictive tool, aiding high temperature forming applications. It was seen that the model was satisfactory at all deformation conditions except for the deformation temperature of 600 °C. In order to improve the predictive capability, the model was extended with a corrective term for predictions at temperatures below 700 °C. The accuracy of the model was displayed with reasonable agreement, resulting in error levels of less than 5% at all deformation temperatures.

Keywords: severe plastic deformation; titanium; equal channel angular extrusion/pressing; high temperature; ultra-fine grained; Johnson-Cook model

1. Introduction

The advent of next generation materials with ultra-fine grains and nanostructures has led to further improvement of mechanical properties. Titanium and its alloys typically find use in various industries, including aerospace, defense, biomedical, energy, and automotive. In this respect, commercial purity titanium (CP Ti) has also received considerable attention due to the opportunity presented by remarkable combinations of strength and ductility by severe plastic deformation (SPD).

As a promising severe plastic deformation (SPD) method, equal channel angular extrusion/pressing (ECAE/P) can generate ultra-fine grained (UFG) structures with high yield strength, and ultimate tensile strength and accompanied by moderate ductility in various studies. The influence of ECAE routes on the microstructure and mechanical properties of CP Ti was investigated [1]. It was found that processing routes are effective in dictating the resulting grain morphology and structural refinement. Another study focused on the critical parameters of ECAE processing as a practical method for grain refinement [2]. Fan *et al.* [3] processed titanium using two-step SPD, consisting of eight passes of ECAE and cold rolling at room and liquid nitrogen temperature. Subsequent cold rolling of ECAE processed specimens led to further refinement of the microstructure, leading to strength levels higher than those of Ti-6Al-4V [4]. A similar work on post-ECAE rolling was also demonstrated in Zhu *et al.* [5]. Furthermore, evolution of crystallographic texture and anisotropy of post-ECAE rolled Ti was another topic of study where the best mechanical characteristics providing high ultimate tensile strength and ductility were revealed in the rolled flow plane samples, strained perpendicular to the rolling direction [6]. Recently, a comparative hardness study was conducted on CP and UFG Ti, indicating 2.5 times higher values for the latter, along with a more uniform microstructure after SPD [7]. As an interesting contribution, Segal [8] analyzed the commercialization of the ECAE process and discussed the optimization of ECAE process by control of contact friction, the channel geometry, strain/strain rate, billet shape, and punch/tool pressures.

In addition to the investigation of processing-structure-property relations, effective use of UFG materials requires efforts into the modeling of the mechanical behavior. For instance, processing of UFG materials requires the estimation of parameters to be applied during post-SPD deformation, including, but not limited to, rolling or forging. Therefore, flow stress characterization and modeling of deformation mechanics under high-temperature conditions is a critical topic, but has rarely been investigated for UFG materials. For the case of UFG Ti, a majority of the studies concentrated on high-temperature mechanical behavior and microstructural characterizations. Hoseini *et al.* [9] investigated the annealing behavior of UFG Ti, where thermal stability up to 450 °C was demonstrated. Long *et al.* [10] probed the mechanical behavior of UFG Ti in a wide temperature range by demonstrating the compressive deformation response from −196 to 600 °C. Recently, Meredith and Khan [11,12] have studied the mechanical properties and texture evolution of severely deformed titanium, at strain rates from 0.0001 to 2000 s^{-1} and temperatures from −196 to 375 °C.

On the modeling front, most investigations considered high temperature flow behavior prediction of coarse-grained Ti. Since the material flow behavior during hot deformation is complex, hardening and softening mechanisms are affected by strain rate as well as temperature. Thus, numerous research efforts have focused on the influence of strain rate and temperature on the flow stress using various constitutive models. A case on commercial purity Ti was presented using an Arrhenius type equation to propose constitutive equations at elevated temperatures up to 700 °C [13]. In another study on pure Ti, Zhang *et al.* [14] applied a model based on the Fields-Backofen equation to predict the tensile behavior up to 600 °C. A similar approach was followed to model the flow stress behavior of commercial pure titanium sheet at temperatures ranging from 350 to 500 °C [15]. Furthermore, neural network prediction of flow stress of a titanium alloy was investigated by Ping *et al.* [16]. Hyperbolic sine function based on the unified viscoplasticity theory was also utilized to model the flow behavior of a beta titanium alloy during hot deformation [17]. Another approach of simulating plastic deformation is proposed by Johnson and Cook [18] and has been utilized for modeling titanium alloys at elevated temperatures [19].

In spite of several studies on UFG Ti, constitutive modeling for describing the hot deformation characteristics of this material needs further investigation. Apart from recent attempts by Sajadifar and Yapici [20–22] considering the flow stress prediction of Ti subjected to eight passes ECAE, modeling of severely deformed materials in the high temperature regime has been a less frequent topic. In the present study, isothermal compression of ECAE processed CP titanium has been carried out at various temperatures and strain rates to characterize the flow behavior during hot deformation. The material behavior at high temperatures is predicted by introducing a modified Johnson-Cook model.

2. Materials and Experimental Procedures

The as-received commercial purity grade 2 Ti was received in bar form, with the chemical composition of 0.008% C, 0.041% Fe, 0.002% H, 0.006% N, 0.150% O and balance Ti represented in weight percent. The bars were coated with a graphite base lubricant before extrusion and were heated in a furnace to the deformation temperature of 300 °C where they were held for 1 h before extrusion. Finally, they were transferred to the 25.4 mm × 25.4 mm cross section, 90° angle ECAE die, which was preheated to 300 °C. Extrusion took place at a rate of 1.27 mm/s. Eight ECAE passes were performed following route E, accumulating a total strain of 9.24 in the as-processed material [23]. Route E was selected as the ECAE processing route, resulting in the largest fully worked region in a given billet with a high volume fraction of high-angle grain boundaries [24]. Route E consists of an alternating rotation of the billet by +180° and +90°, around its long axis, between successive passes. Following each extrusion pass, the billets were water quenched to maintain the microstructure achieved during ECAE. Lowest possible processing temperatures were crucial in preventing possible recrystallization and partly achieved using the sliding walls concept [8].

In exploring the hot deformation behavior of ECAE processed pure Ti, hot compression experiments were performed. The compression specimens were electro-discharge machined (EDM) in a rectangular block shape, 4 mm × 4 mm × 8 mm, with compression axis parallel to the extrusion direction. All samples were ground and polished to remove major scratches and eliminate the influence of a residual layer from EDM. The compression tests were conducted under isothermal conditions at three different strain rates of 0.001, 0.01, and 0.1 s^{-1} and at temperatures of 600, 700, 800, and 900 °C. All specimens were heated up to the deformation temperature and then the samples were deformed in a single loading step. The reduction in height at the end of the compression tests was 60% (true strain: 0.9) to avoid barreling and to capture the effect of both dynamic recovery and recrystallization on deformation behavior. In addition, lubrication with graphite was used during hot compression tests to decrease friction effects and minimize barreling [25]. The mechanical experiments were conducted inside a temperature-controlled furnace mounted on an Instron mechanical testing frame with uniformly heated samples having constant temperature profiles throughout the tests.

3. Results and Discussion

3.1. Effects of Temperature and Deformation Rate on the Microstructural Evolution

Increase of deformation temperature and decrease of deformation rate caused the growth of recrystallized grains in severely deformed titanium, as represented in Figure 1. Effect of deformation temperature on grain growth was observed to be more remarkable than that of deformation rate. At 900 °C, there is significant energy to promote nucleation and rapid growth of dynamically recrystallized grains. Deforming samples at 600 °C and 900 °C for longer periods led to a coarser structure since dynamically recrystallized grains had enough time to grow after nucleation.

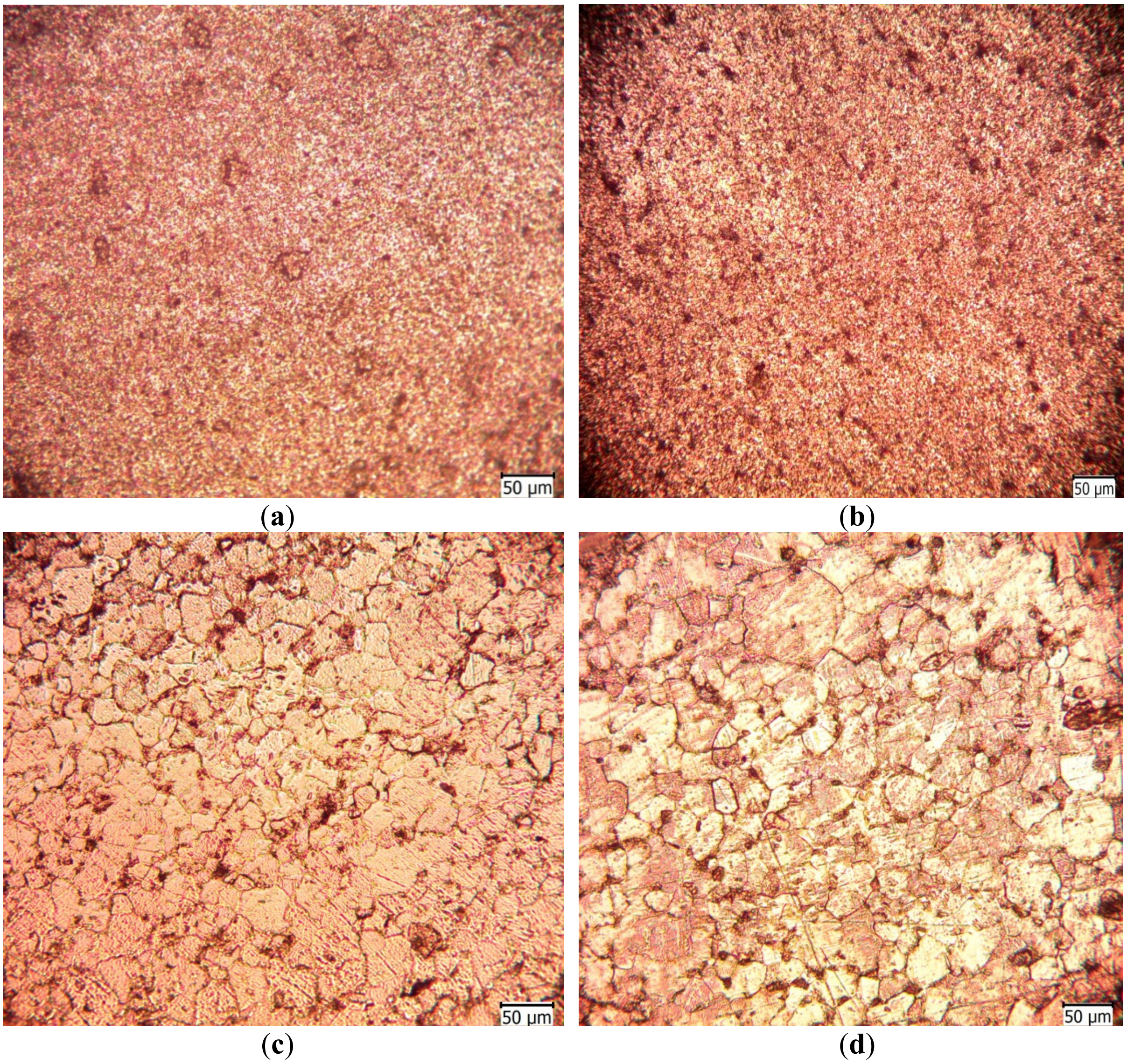

Figure 1. Microstructure of severely deformed titanium followed by hot compression test at (**a**) 600 °C-0.1s^{-1}, (**b**) 600 °C-0.001s^{-1}, (**c**) 900 °C-0.1s^{-1}, (**d**) 900 °C-0.001s^{-1}.

3.2. Constitutive Equation for the Modified Johnson-Cook Model

Flow stress during hot deformation is dependent on strain (ε), strain rate ($\dot{\varepsilon}$), and temperature (*T*), which can be described by the following function:

$$\sigma = f\left(\varepsilon, \dot{\varepsilon}, T\right) \quad (1)$$

The Johnson-Cook (JC) and its modified models are utilized in different materials to predict their flow stress behavior at elevated temperature [18]. The modified JC equation for hot compression is as follows [26]:

$$\sigma = \left(\sigma_P + B\left(T\right)\varepsilon^{n(T)}\right)\left[1 + C\left(\varepsilon, T\right)\ln\left(\frac{\dot{\varepsilon}}{\dot{\varepsilon}_0}\right)\right] \quad (2)$$

B(*T*) and *n*(*T*) are material constants, which are dependent on deformation temperature. *C*(ε,*T*) is the material constant that is a function of both deformation temperature and strain. $\dot{\varepsilon}_0$ is the reference strain rate. The lowest strain rate (0.001 s^{-1}) is selected as the reference strain rate [26].

3.3. Calculation of B(T), n(T) and C(ε,T)

For the strain rate ($\dot{\varepsilon}$) of 0.001 s^{-1}, Equation (2) can be written as:

$$\sigma = \left(\sigma_P + B\left(T\right)\varepsilon^{n(T)}\right) \quad (3)$$

where σ_P is the peak stress. Taking the logarithm of Equation (3), gives:

$$\ln\left(\sigma_P - \sigma\right) = \ln\left[-B\left(T\right)\right] + n\left(T\right)\ln\left(\varepsilon\right) \quad (4)$$

The values of *n* and *B* can be obtained from Equation (4), according to the slope and intercept of the lines (Figure 2), respectively. The linear relationship was seen to be better at higher deformation temperatures in comparison with that of lower temperatures. This could be attributed to the stability of the UFG structure at lower deformation temperatures bringing higher discrepancy at 600 °C and 700 °C. The values of *n* and *B* are presented in Table 1.

Table 1. The values of *B* and *n* under different temperatures and at a strain rate of 0.001 s^{-1}.

Material Constants	600 °C	700 °C	800 °C	900 °C
B(*T*), MPa	−60.099	−11.806	−1.696	−1.995
n(*T*)	4.311	3.251	1.319	0.123

With the substitution of *n*(*T*) and *B*(*T*) into Equation (2), respective values of *C*(ε,*T*) can be calculated under various deformation conditions. The values of *C*(ε,*T*) *versus* strain for different deformation conditions are obtained by linear fitting (Figure 3). As presented in Table 2 for selected true strain levels. For the sake of brevity, figures demonstrating the relation for the other deformation temperatures are not presented here.

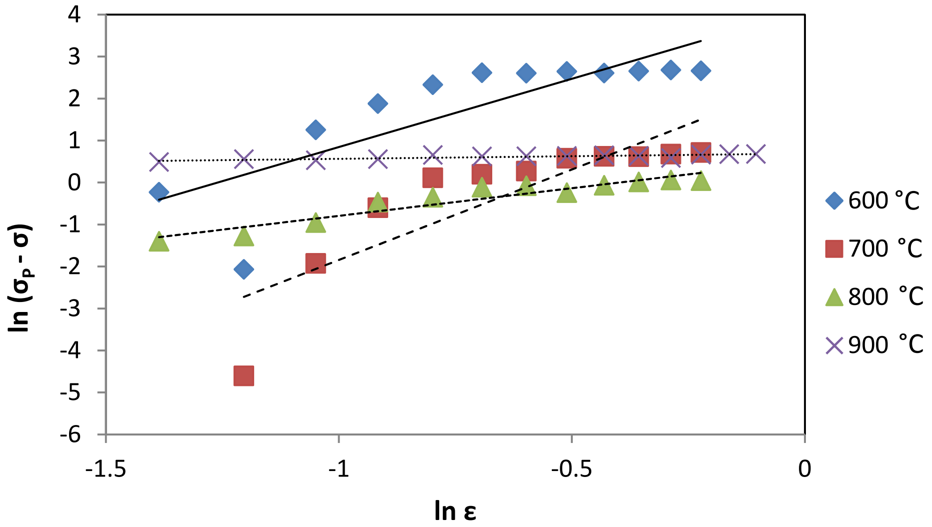

Figure 2. Relationship between ln(σ_P −σ) and ln(ε) at various temperatures and at a strain rate of 0.001 s^{-1}.

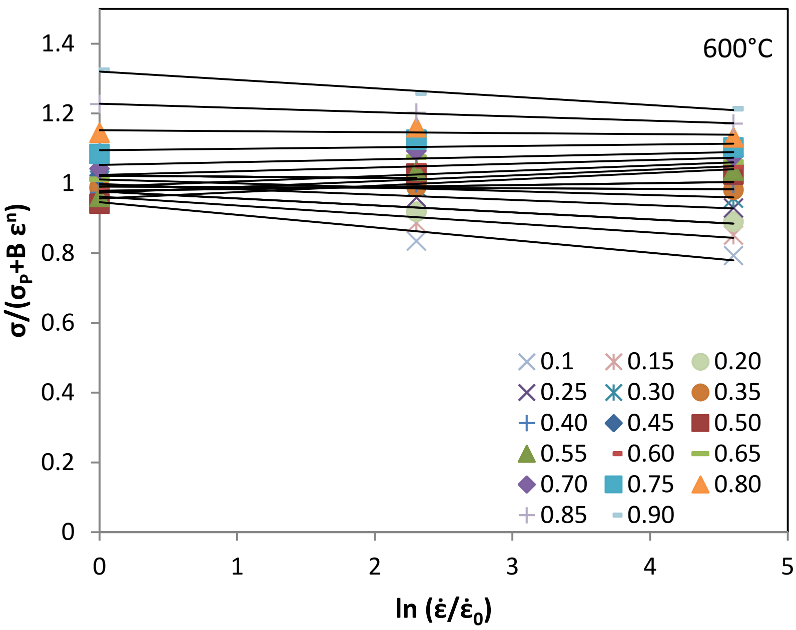

Figure 3. Relationship between $\dfrac{\sigma}{\left[\sigma_P + B(T)\varepsilon^{n(T)}\right]}$ and $\ln\left(\dfrac{\dot{\varepsilon}}{\dot{\varepsilon}_0}\right)$.

Table 2. The values of *C* at different deformation strain levels and temperatures.

Strain	600 °C	700 °C	800 °C	900 °C
0.20	−0.0201	−0.013	0.0005	−0.013
0.40	0.0055	−0.0005	0.0016	−0.0005
0.60	0.015	−0.0162	−0.0019	−0.0162
0.80	−0.0029	−0.0265	−0.0035	−0.0265

3.4. Prediction of Flow Stress by the Modified Johnson-Cook Modeling

The flow stress behavior of ECAE processed pure Ti can be predicted by applying $B(T)$, $n(T)$ and $C(\varepsilon,T)$ to Equation (2), as demonstrated in Figure 4. This model is precise in predicting the flow stress at all deformation conditions except at a temperature of 600 °C. At lower deformation temperatures and higher deformation rates, the severely deformed microstructure is partly retained, and as such, the model may lose its accuracy in determining the actual softening behavior.

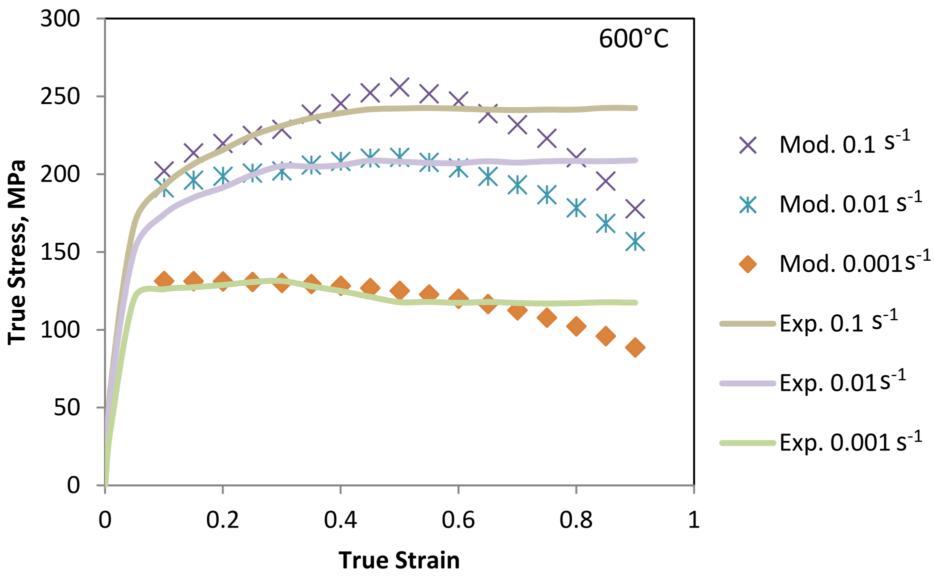

(a)

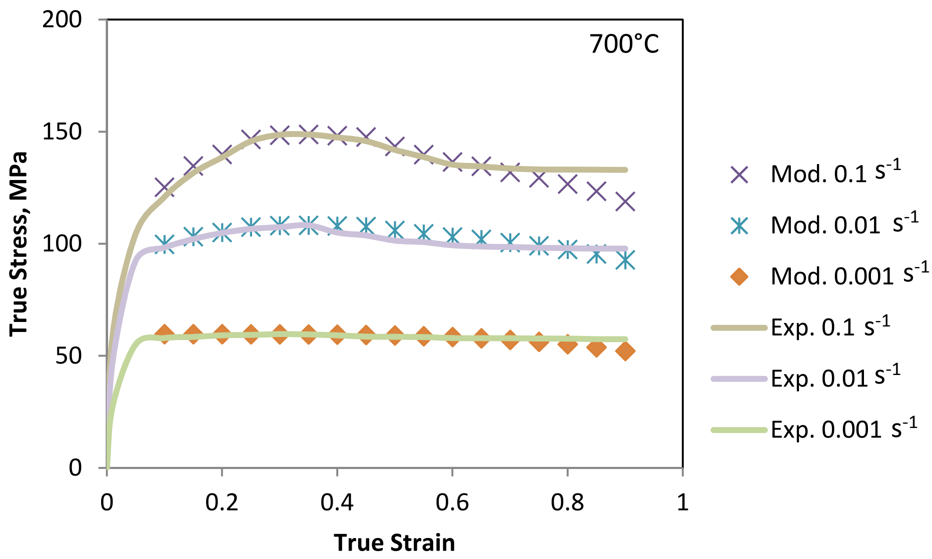

(b)

Figure 4. *Cont.*

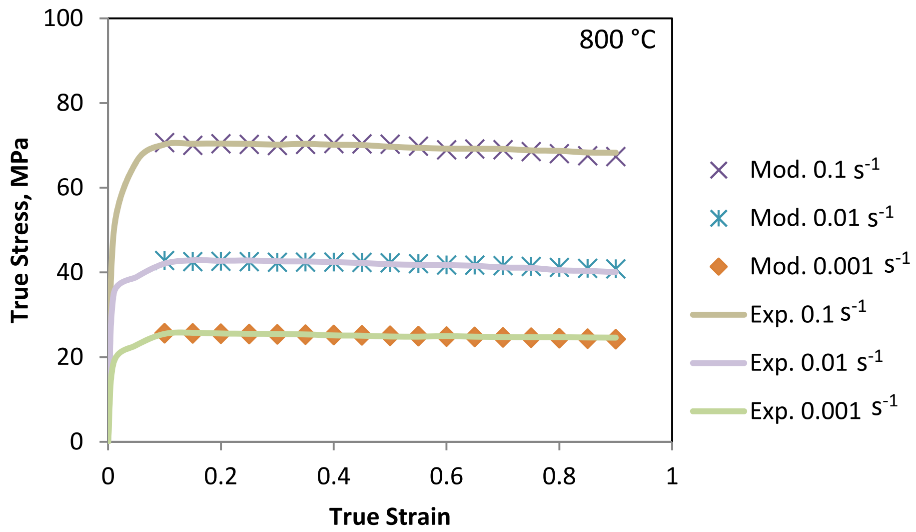

(**c**)

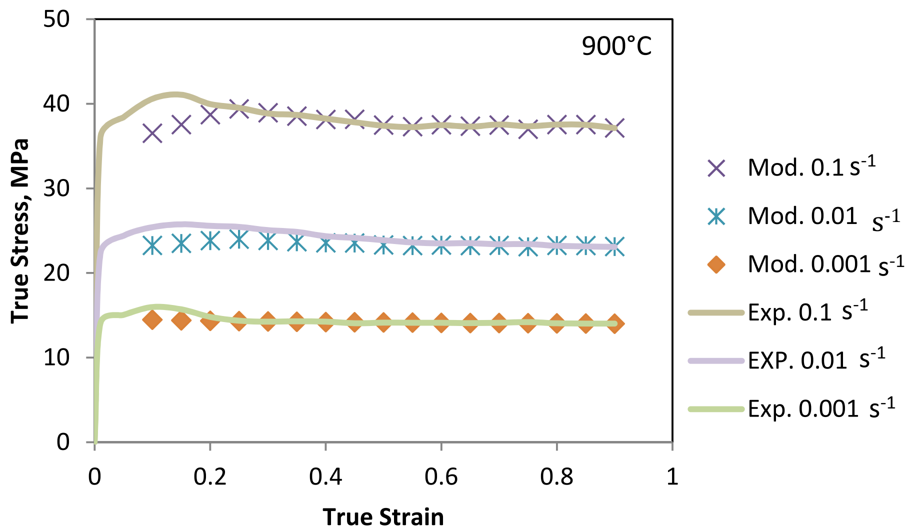

(**d**)

Figure 4. Comparison among model predictions and experimental results at: (**a**) 600 °C, (**b**) 700 °C, (**c**) 800 °C, (**d**) 900 °C.

Furthermore, it is worth noting that the difference between the simulated and experimental data is higher with increasing strain at 600 °C. Here, the modeled flow stress curves generally reach a peak and then decrease sharply, which is a pronounced characteristic of dynamic recrystallization. However, few experimental flow stress curves feature a peak followed by an immediate plateau. This is a well-known behavior of dynamic recovery and can be observed at the lowest deformation temperature.

3.5. Extension of the Johnson-Cook Model for Prediction of ECAE Processed Ti with a Corrective Term

When modeling the deformation at 600 °C, there is a considerable discrepancy between the experimental and model flow responses especially after the peak stress. The variation of the material constants, $n(T)$ and $B(T)$, as a function of temperature is plotted in Figure 5 exhibiting strong dependence on the deformation temperature. It is worth noting that $n(T)$ increases with decrease of deformation temperature. Moreover, it was seen that the absolute value of $B(T)$ shows a considerable increase with decrease of deformation temperature. However, at higher temperatures, $B(T)$ is fairly constant and can be considered to be independent of temperature. With the increase of deformation temperature, a similar behavior for $B(T)$ and $n(T)$ was reported for modeling the high temperature behavior of an aluminum alloy [26].

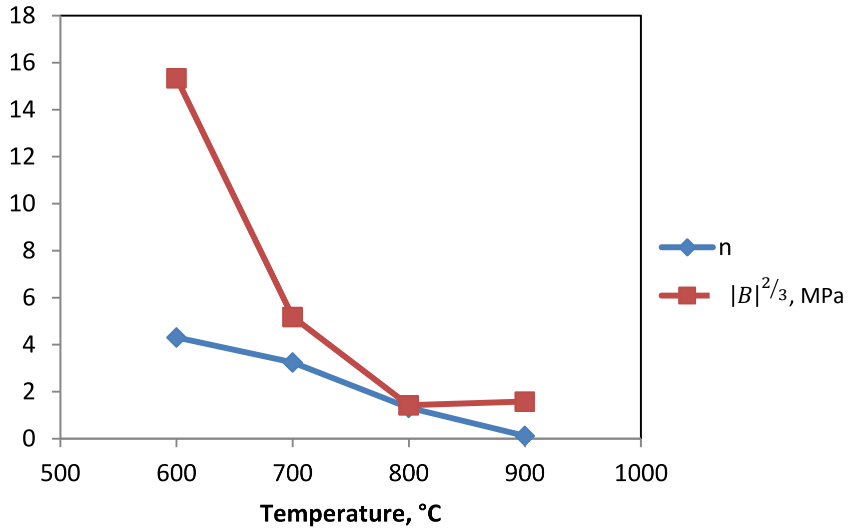

Figure 5. Deformation temperature *versus* n and $|B|^{2/3}$.

Another important factor affecting the predictions of this model is the amount of true strain. As can be observed in Figure 4a, agreement of the model with the experimental data gets worse from peak strain up to a true strain of 0.9. Considering that the error levels are comparably larger for deformation at 600 °C, a new term accounting for this behavior is added to Equation (2). This corrective term can be formulated as:

$$\text{Corrective Term} = \frac{\left(n(T)+\varepsilon\right)\left(\sigma_P \cdot \varepsilon^{n(T)}\right)}{\left|B(T)\right|^{\frac{2}{3}}} \tag{5}$$

The corrective term depends on the degree of deformation temperature via the inclusion of the material constants, $n(T)$ and $B(T)$. With the dependence of corrective term on true strain, flow stress levels are expected to remain constant and a plateau behavior can be obtained. The modified flow response prediction at the lowest deformation temperature of 600 °C is shown in Figure 6 demonstrating better agreement with the experimental curve.

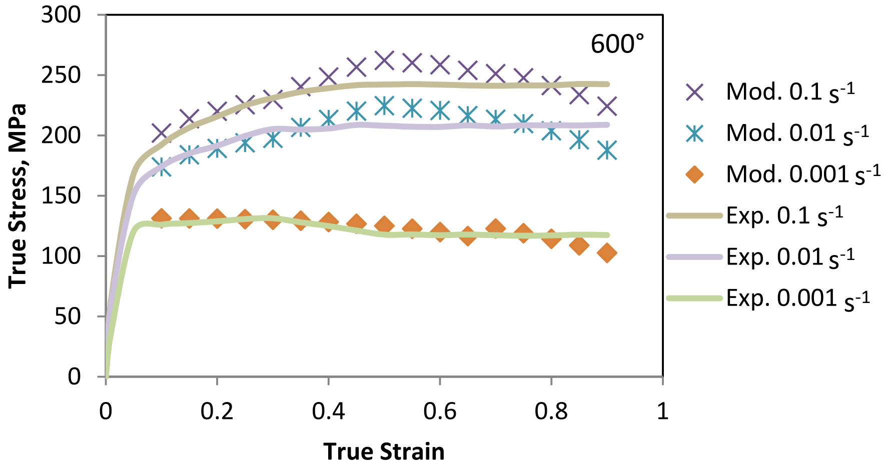

Figure 6. Comparison between improved model predictions and experimental results at 600 °C.

3.6. Verification of the Model

In order to verify the accuracy of the applied constitutive model, the deviations between the predicted stress (σ_P) and experimental stress (σ_E) values were obtained as:

$$E(\%) = \left| \frac{\sigma_P - \sigma_E}{\sigma_E} \right| \times 100 \tag{6}$$

Figure 7 demonstrates the mean error values for the modeling approach based on the modified JC equation. It can be seen that the highest error level is less than 5% in all cases indicating reasonable agreement. In a separate study, models based on Arrhenius and dislocation density based formulations were employed for modeling the behavior of ECAE processed Ti in the warm to hot working regime. It can be seen that the error levels obtained using the current model is comparably less than those reported in [20,22].

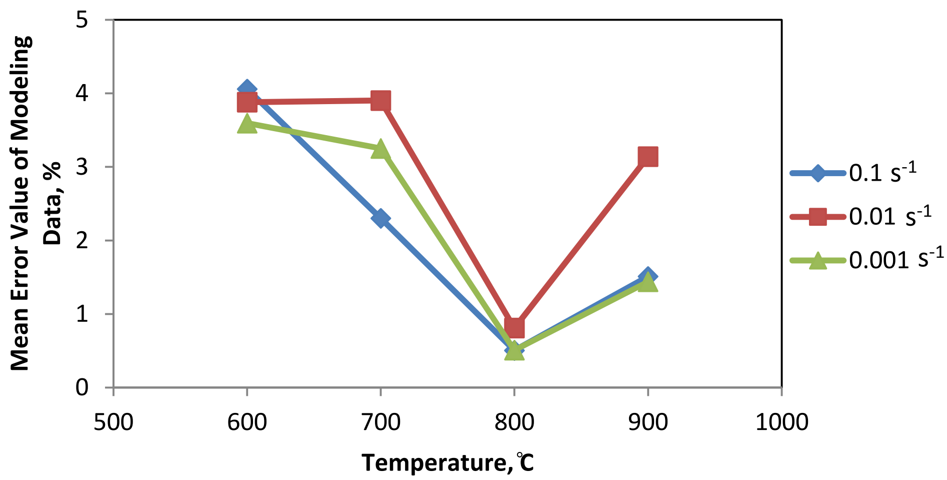

Figure 7. Mean error of the model for various deformation conditions.

Although both the modified JC and dislocation density based models exhibit decent predictive capability at relatively higher temperatures, their accuracy depends on how the active softening mechanisms are treated according to the deformation temperature. Another assumption of these constitutive models is that, they typically consider coarse grained microstructures. However, it was mentioned that the average grain size of UFG titanium remained less than 3.5 μm at 600 °C [9]. This finding was also confirmed in a different study [20,22]. On the other hand, the microstructure of ECAE processed Ti followed by hot compression tests (above 700 °C) contained grains with average size over 15 μm [22]. Therefore, the relatively fine grain size at lower temperatures could lead to the higher error levels observed in the prediction of the flow response at 600 °C.

4. Conclusions

The hot deformation behavior of ECAE processed pure Ti was studied by isothermal compression tests in temperatures ranging from 600 °C to 900 °C and strain rates ranging from 0.001 s^{-1} to 0.1 s^{-1}. The modified Johnson Cook model was utilized to predict the flow behavior of ECAE processed pure Ti leading to a satisfactory agreement with experimental data in all cases except 600 °C. The model is extended with a corrective term to improve the error levels at lower temperatures. This resulted in the highest error level to remain less than 5%, pointing to the probable use of the presented model in predicting the compressive response of ECAE processed Ti at elevated temperatures.

Acknowledgments

The authors would like to acknowledge the support from the European Union Seventh Framework Programme, Marie Curie Career Integration Grant, Project No: 304150, for conducting this investigation.

Author Contributions

G.G. Yapici designed the scope of the paper. S.V. Sajadifar prepared samples and conducted experiments. Both authors analyzed the results and participated in the modeling studies. S.V. Sajadifar wrote the initial draft and G.G. Yapici shaped the manuscript into its final form.

Conflicts of Interest

The authors declare no conflict of interest.

References

1. Stolyarov, V.V.; Zhu, Y.T.; Alexandrov, I.V.; Lowe, T.C.; Valiev, R.Z. Influence of ECAP routes on the microstructure and properties of pure Ti. *Mater. Sci. Eng. A* **2001**, *299*, 59–67.
2. Valiev, R.Z.; Langdon, T.G. Principles of equal channel angular pressing as a processing tool for grain refinement. *Prog. Mater. Sci.* **2006**, *51*, 881–981.
3. Fan, Z.; Jiang, H.; Sun, X.; Song, J.; Zhang, X.; Xie, C. Microstructures and mechanical deformation behaviors of ultrafine-grained commercial pure (grade 3) Ti processed by two-step severe plastic deformation. *Mater. Sci. Eng. A* **2009**, *527*, 45–51.

4. Stolyarov, V.V.; Zhu, Y.T.; Alexandrov, I.V.; Lowe, T.C.; Valiev, R.Z. Grain refinement and properties of pure Ti processed by warm ECAP and cold rolling. *Mater. Sci. Eng. A* **2003**, *343*, 43–50.
5. Zhu, Y.T.; Kolobov, Y.R.; Grabovetskaya, G.P.; Stolyarov, V.V.; Girsova, N.V.; Valiev, R.Z. Microstructures and mechanical properties of ultrafine-grained Ti foil processed by equal-channel angular pressing and cold rolling. *J. Mater. Res.* **2003**, *18*, 1011–1016.
6. Yapici, G.G.; Karaman, I.; Maier, H.J. Mechanical flow anisotropy in severely deformed pure titanium. *Mater. Sci. Eng. A* **2006**, *434*, 294–302.
7. Sanosh, K.P.; Balakrishnan, A.; Francis, L.; Kim, T.N. Vickers and Knoop Micro-hardness Behavior of Coarse-and Ultrafine-grained Titanium. *J. Mater. Sci. Technol.* **2010**, *26*, 904–907.
8. Segal, V.M. Engineering and commercialization of equal channel angular extrusion (ECAE). *Mater. Sci. Eng. A* **2004**, *386*, 269–276.
9. Hoseini, M.; Pourian, M.H.; Bridier, F.; Vali, H.; Szpunar, J.A.; Bocher, P. Thermal stability and annealing behaviour of ultrafine grained commercially pure titanium. *Mater. Sci. Eng. A* **2012**, *532*, 58–63.
10. Long, F.W.; Jiang, Q.W.; Xiao, L.; Li, X.W. Compressive deformation behaviors of coarse- and ultrafine-grained pure titanium at different temperatures: a comparative study. *Mater. Trans.* **2011**, *52*, 1617–1622.
11. Meredith, C.S.; Khan, A. The microstructural evolution and thermo-mechanical behavior of UFG Ti processed via equal channel angular pressing. *J. Mater. Process. Technol.* **2015**, *219*, 257–270.
12. Meredith, C.S.; Khan, A. Texture evolution and anisotropy in the thermo-mechanical response of UFG Ti processed via equal channel angular pressing. *Int. J. Plasticity* **2012**, *30–31*, 202–217.
13. Zeng, Z.; Jonsson, S.; Zhang, Y. Constitutive equations for pure titanium at elevated temperatures. *Mater. Sci. Eng. A* **2009**, *505*, 116–119.
14. Zhang, Z.Y.; Yang, H.; Li, H.; Ren, N.; Wang, D. Quasi-static tensile behavior and constitutive modeling of large diameter thin-walled commercial pure titanium tube. *Mater. Sci. Eng. A* **2013**, *569*, 96–105.
15. Tsao, L.C.; Wu, H.Y.; Leong, J.C.; Fang, C.J. Flow stress behavior of commercial pure titanium sheet during warm tensile deformation. *Mater. Des.* **2012**, *34*, 179–184.
16. Ping, L.; Kemin, X.; Yan, L.; Jianrong, T. Neural network prediction of flow stress of Ti–15–3 alloy under hot compression. *J. Mater. Process. Technol.* **2004**, *148*, 235–238.
17. Wang, Z.; Qiang, H.; Wang, X.; Wang, G. Constitutive model for a new kind of metastable beta titanium alloy during hot deformation. *Trans. Nonferrous Metals Soc. China* **2012**, *22*, 634–641.
18. Johnson, G.R.; Cook, W.H. A constitutive model and data for metals subjected to large strains, high strain rates and high temperatures. In Proceedings of the 7th International Symposium on Ballistics, The Hague, The Netherlands, 19–21 April 1983; pp. 541–547.
19. Khan, A.S.; Suh, Y.S.; Kazmi, R. Quasi-static and dynamic loading responses and constitutive modeling of titanium alloys. *Int. J. Plasticity* **2004**, *20*, 2233–2248.
20. Sajadifar, S.V.; Yapici, G.G. Workability characteristics and mechanical behavior modeling of severely deformed pure titanium at high temperatures. *Mater. Des.* **2014**, *53*, 749–757.
21. Sajadifar, S.V.; Yapici, G.G. Hot Deformation Behavior of Ultra-fine Grained Pure Ti. *Adv. Mater. Res.* **2014**, *829*, 10–14.

22. Sajadifar, S.V.; Yapici, G.G. Elevated temperature mechanical behavior of severely deformed pure titanium. *J. Mater. Eng. Perform.* **2014**, *23*, 1834–1844.
23. Segal, V.M. Materials processing by simple shear. *Mater. Sci. Eng. A* **1995**, *197*, 157–164.
24. Purcek, G.; Yapici, G.G.; Karaman, I.; Maier, H.J. Effect of commercial purity levels on the mechanical properties of ultrafine-grained titanium. *Mater. Sci. Eng. A* **2011**, *528*, 2303–2308.
25. Li, L.X.; Peng, D.S.; Liu, J.A.; Liu, Z.Q. An experiment study of the lubrication behavior of graphite in hot compression tests of Ti-6Al-4V alloy. *J. Mater. Process. Technol.* **2001**, *112*, 1–5.
26. Lin, Y.C.; Li, Q.F.; Xia, Y.C.; Li, L.T. A phenomenological constitutive model for high temperature flow stress prediction of Al-Cu-Mg alloy. *Mater. Sci. Eng. A* **2012**, *534*, 654–662.